Solar-Terrestrial Physics. 2022. Vol. 8. Iss. 3. P. 69–75. DOI: 10.12737/stp-83202211. © 2022 Legostaeva Yu.K., Shindin A.V., Grach S.M. Published by INFRA-M Academic Publishing House

UDC 533.951
DOI: 10.12737/stp-83202211

Received March 31, 2022
Accepted August 02, 2022

RESPONSE OF IONOSPHERIC ELECTRON DENSITY PROFILE TO THE ACTION OF POWERFUL HF RADIO-WAVE RADIATION

Yu.K. Legostaeva
N.I. Lobachevsky State University of Nizhny Novgorod, Nizhny Novgorod, Russia, julilegostaeva@gmail.com

A.V. Shindin
N.I. Lobachevsky State University of Nizhny Novgorod, Nizhny Novgorod, Russia, shindin@rf.unn.ru

S.M. Grach
N.I. Lobachevsky State University of Nizhny Novgorod, Nizhny Novgorod, Russia, sgrach@rf.unn.ru

Abstract. Using electron density and temperature equations, we have modeled the dynamics of the electron density profile in the ionosphere due to the expulsion of plasma from localization regions of plasma waves, pumped by high-power HF radio waves, i.e. wave reflection and upper hybrid resonance regions. Causes of the ionospheric plasma expulsion are an increase in the gas-kinetic pressure due to the ohm heating of electrons by plasma waves, and the high-frequency pressure of plasma waves (ponderomotive expulsion). We have established that the ponderomotive expulsion develops more rapidly and is responsible for the formation of local regions of plasma density depletion near plasma resonances, whereas the gas-kinetic pressure increase is responsible for the formation of lower-density region, which is slower in time and more extended and smoother in height. The results obtained qualitatively agree with the data from the experiment conducted at the HAARP facility in 2014.

Keywords: ionosphere, electron heating, powerful HF radiation, ponderomotive expulsion, profile modification.

INTRODUCTION

Plasma expulsion from the upper hybrid resonance (UHR) region of a powerful radio wave (pump wave, PW), where $f_{pe}^2 = f_0^2 - f_{He}^2$, was found in the experiments on studying disturbances of the ionospheric volume pumped by powerful HF radio-wave of ordinary polarization by the multifrequency Doppler sounding (MDS) at the SURA facility in the 1980th [Vaskov et al., 1986]. Here f_0, f_{pe}, f_{He} are the PW frequency, electron plasma, and cyclotron frequencies respectively. These results directly confirmed theoretical ideas about the important role of processes in the UHR region in exciting artificial ionosphere turbulence [Vas'kov, Gurevich, 1976; Grach, Trakhtengertz, 1975; Grach et al., 1981]. Later, similar experiments found plasma expulsion from a PW reflection region, where $f_0 = f_{pe}$ [Berezin et al., 1991], which occurred earlier than that from the UHR region. This expulsion was weaker and disappeared (or noticeably weakened) after the development of processes in the UHR region. The latter suggests that the plasma expulsion from the PW reflection region is connected with the rapid (in fractions of a second) excitation of plasma (Langmuir) waves due to the development of a ponderomotive parametric instability at the initial stage of pumping. Slower processes in the UHR region (thermal parametric and resonance instabilities), which lead to the occurrence of small-scale irregularities, extended along the magnetic field, and upper hybrid waves, shield the reflection point, and the pump energy is injected into plasma in the UHR region.

The effect of plasma expulsion from the PW reflection and UHR regions occurs at sufficiently high effective PW powers: 150–250 MW at different f_0 at the Sura facility [Vaskov et al., 1986; Berezin et al., 1991; Grach et al., 1997], 280 MW at the EISCAT/heating facility (Tromsø, Norway) [Lobachevsky et al., 1992], 400 MW at the HAARP facility (Alaska, the USA) [Shindin et al., 2021]. At low PW powers, there are no expulsion effects, despite the effective excitation of artificial turbulence in the PW reflection and UHR regions. Moreover, when a PW frequency is close to the electron cyclotron frequency harmonics ($f_0 \approx nf_{He}$), the development of disturbances in the UHR region is noticeably weakened and slowed down. At the same time, the plasma expulsion from the reflection region is observed for a longer time [Lobachevsky et al., 1992], and the profile modification changes significantly [Shindin et al., 2021].

The MDS method involves using a set of test radio waves with different frequencies. Analyzing phase characteristics of the test signals reflected from a disturbed region allows us to reconstruct the vertical electron density profile $N_e(z)$ and hence the relative variation in the electron density $\frac{\Delta N_e}{N_0} = \frac{N_e - N_0}{N_0}$. The altitude resolution of the reconstructed profile directly depends on the frequency shift between "neighboring" test waves, and the frequency range of the test waves determines the range of heights in the reconstructed profile. In the first MDS experiments [Vaskov et al., 1986; Lobachevsky et al., 1992; Grach et al., 1997; Berezin et al., 1991], the number of the these waves did not exceed eight, in some cases it was twelve. Since 2006, a modi-

fied MDS method has been used [Sergeev et al., 2007], which makes it possible to significantly improve the altitude resolution of the reconstructed profile as well as to trace its temporal evolution. This is achieved due to special combined modes of heating facility radiation, used for ionosphere pumping and sounding [Sergeev et al., 2007; Grach et al., 2016]. The probe (sounding) radiation in this case is a sequence of short (20–200 μs) radio pulses. Recording ionospherically reflected radio pulses with modern wide-band receivers enables identification of their spectral components against the noise background in a bandwidth to 1 MHz, these components serve as test waves. The use of regularization algorithms makes it possible to correctly account for the geomagnetic field effect when solving the inverse problem. As a result, the method provides the following parameters of the reconstructed profile $N_e(z, t)$: ~50 m altitude resolution, ~30 km altitude range, ~100–200 μs time resolution. Experiments carried out with the SURA facility with the new method have confirmed the results of earlier experiments: the initial plasma expulsion from the reflection region, the subsequent shielding of the reflection region, and the slower development (along with UHR turbulence) of plasma expulsion from the UHR region [Shindin et al., 2012].

The expulsion effects and the ionospheric electron density profile modification have been studied theoretically in [Vaskov, Dimant, 1989; Grach et al., 1989; Dimant, 1989]. These effects can be associated both with the ponderomotive (average HF) pressure of plasma waves and with an increase in the gas-kinetic pressure of plasma due to heating of electrons by plasma waves. Grach et al. [1998] have found that in the SURA experiment, by the end of minute pumping cycles, the expulsion effect prevailed due to the increase in the gas-kinetic pressure. Plasma waves, in turn, appeared at heights of plasma resonances (reflection and UHR regions) due to excitation of parametric instabilities under the influence of a powerful radio wave on the ionosphere.

In 2014, a series of experiments on the modification of the ionospheric electron density profile, using multifrequency Doppler sounding by the technique developed at the Sura facility, was carried out with the HAARP heating facility (Alaska, the USA), whose power is about 10 times higher than the power of the Sura facility [Sergeev et al., 2016; Shindin et al., 2021]. It was found that in a number of sessions both expulsion regions (near the reflection point and near the UHR height) were preserved during the entire exposure time (>40 s).

The purpose of this work is to determine the mechanism of formation of the modified electron density profile in the ionosphere, observed in the experiment [Shindin et al., 2021] with the HAARP facility, under the action of a powerful HF radio wave. Section 1 briefly states the results of the HAARP experiment (altitude dependences $\Delta N_e/N_0$) in one of the heating sessions at different instants of time after switching on a PW. Section 2 formulates a system of equations including the thermal conductivity equation taking into account the source of heating by plasma waves and the ambipolar diffusion equation with account of the electron thermodiffusion and ponderomotive pressure.

Section 3 presents the results of calculations within the formulated system for parameters that provide the closest similarity to the empirical data. Section 4 briefly discusses the results.

1. EXPERIMENTAL DATA

In 2014, a series of experiments was conducted with the HAARP heating facility to study the modification of the electron density profile in the ionosphere, using the method developed at the Sura facility. The effective power of the HF radiation was 400 MW, which is much higher than that of Sura. The electron density dependence $\frac{\Delta N_e(z,t)}{N_0} = \frac{N_e(z,t) - N_0}{N_0}$ obtained in one of the experimental sessions (z is the height; t is the time after switching on a PW) is shown in Figure 1 from [Shindin et al., 2021]. The pump wave was switched on at t=0 and switched off at t=45 s. The PW frequency f_0 was 5540 kHz, the true PW reflection height z_r= 237 km, the true UHR height z_{uh}=230 km. Note that in this session the PW frequency was quite far from the multiple cyclotron resonance: $f_0 - 4f_{He} \sim -150$ kHz.

Figure 1 displays the relative amount of the expulsed plasma at different time points; z_r and z_{uh} are the initial heights of the reflection point and UHR respectively. Regions of the decreased electron density are seen to develop both near the height of the reflection point z_r, where $f_0=f_{pe}$, and near the height of UHR ($z=z_{uh}$), where

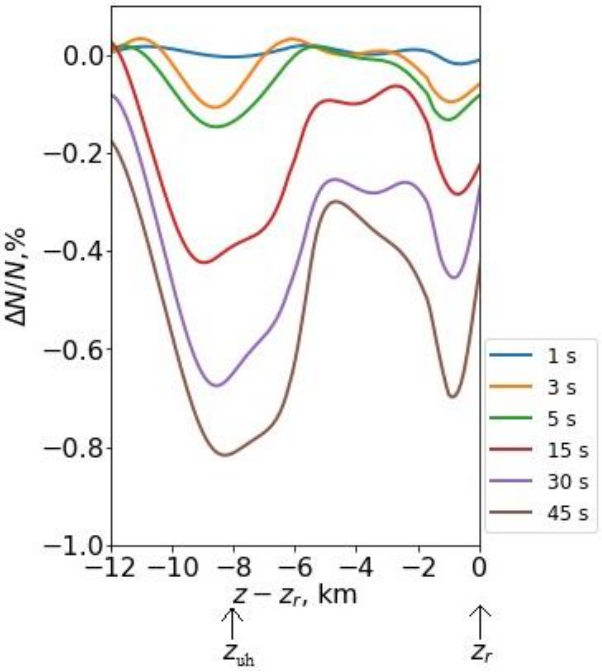

Figure 1. Relative electron density variations $\Delta N_e/N_0=[N_e(t)-N_e(0)]/N_e(0)$ as a function of height at 1, 3, 5, 15, 30, 40 s of heating. The PW frequency f_0=5540 kHz, $z-z_r$=0 corresponds to the position of the reflection point z_r. The arrows show the initial heights of the PW reflection z_r and upper hybrid resonance z_{uh}

$f_{pe}^2 = f_0^2 - f_{He}^2$. As the pumping time t increases, the electron density decreases more slowly between these heights, and this trend persists throughout the exposure time (45 s).

2. THEORETICAL MODEL. BASIC EQUATIONS

When an O-polarization powerful radio wave (pump waves) falls on the ionosphere in a direction close to vertical, plasma waves are excited in the region of plasma resonances. According to present-day views (see, e.g., [Grach et al., 2016]), there are two regions where the contribution of the PW energy to ionospheric plasma is effective: the first is near the PW reflection point ($f_0=f_{pe}$, $z=z_r$), where a ponderomotive parametric instability develops most rapidly (in a matter of milliseconds), and the second is near the PW UHR height ($f_0^2=f_{pe}^2+f_{He}^2$, $z=z_{uh}$), where a thermal parametric instability is excited more slowly (for several seconds). Due to the pondermotive parametric instability, Langmuir waves are excited, while the thermal parametric instability is responsible for the excitation of upper hybrid waves and small-scale plasma density irregularities, elongated along the geomagnetic field. The plasma waves in the reflection and UHR regions have a low group velocity; they effectively accumulate and dissipate almost locally in the excitation region. The sharply inhomogeneous accumulation of plasma waves in height should lead to intense ejection of electrons from the resonance region by the pondermotive force (Miller force) [Dimant, 1989; Grach et al., 1989; Vaskov, Dimant, 1989]. Furthermore, the collisional dissipation of plasma waves leads to additional heating of electrons, which also causes plasma expulsion from the resonance region due to a gas-kinetic pressure increase [Gurevich, Schwarzburg, 1973; Dimant, 1989].

In conditions of the experiments at the EISCAT/heating, Sura, and HAARP facilities, the geomagnetic field is almost vertical ($\theta=\measuredangle z$ **B**=12°, 18.5°, and 14° respectively); moreover, the antenna patterns of the facilities are quite wide (the horizontal size of the disturbed region at altitudes of ~230 km is ~50 km). Since the ionospheric plasma transport in the direction transverse to the geomagnetic field **B** is significantly slowed down, we can assume that the plasma expulsion from the regions of the PW energy contribution occurs along the magnetic field.

At sufficiently long times ($t_{>1/\nu_i}$, ν_i is the frequency of ion collisions) and at large scales ($\Delta z>l_e$, the mean free path of electrons), the plasma motion in this direction is described by the equation [Gurevich, Schwarzburg, 1973]

$$\frac{\partial \Delta N}{\partial t} - D_a \cos^2\theta \frac{\partial^2 \Delta N}{\partial z^2} + \frac{\Delta N}{\tau_N} = \\ = \frac{m_e}{m_i}\frac{N_0}{\nu_i}\cos^2\theta \frac{\partial^2 \Phi_e}{\partial z^2} + D_{T_{ea}} \cos^2\theta \frac{N_0}{T_0}\frac{\partial^2 T_e}{\partial z^2}. \quad (1)$$

Here $\Delta N=N-N_0$ is the plasma density perturbation; N_0 is the initial (equilibrium) density; $D_a = \frac{T_e + T_i}{m_i \nu_i}$ is the coefficient of ambipolar plasma diffusion; $\tau_N=(\alpha N_e)^{-1}$ is the electron lifetime; $D_{Tea}=k_T D_a$ is the coefficient of ambipolar thermodiffusion; k_T is the thermodiffusion ratio, in the elementary theory at hand $k_T=1$; m_e, m_i, T_e, T_i are masses and temperatures (in energy units) of electrons and ions; ν_i is the frequency of ion collisions; θ is the angle between the vertical and the geomagnetic field (the temperature and density are redistributed along the magnetic field). In HAARP experiment conditions, θ≈76°, hence $\cos^2\theta=0.94\sim1$. The first term on the right-hand side of Equation (1) is related to the ponderomotive plasma expulsion. Here Φ is the average HF potential (accordingly, the pondermotive force is equal to $-\nabla\Phi$ [Gaponov, Miller, 1958; Pitaevskii, 1960]):

$$\Phi = \frac{e^2 |\mathbf{E}|^2}{4m\omega^2} \approx \frac{W(z)}{2N_0 m_e}, \quad (2)$$

where e is an electron charge; $|\mathbf{E}|^2$ is the integral intensity of a high-frequency electric field; W is the integral (in terms of frequencies ω and wave vectors **k**) energy density of plasma waves: The $W = \frac{1}{8\pi}\int E_{\omega,k}^2 \, d\mathbf{k}\, d\omega$. The PW energy density in the excitation region of plasma waves is small compared to W and can be neglected. The second term on the right-hand side of Equation (1) is related to thermodiffusion — the redistribution of electrons due to variations in electron temperature and hence in gas-kinetic pressure. The behavior of the electron temperature under PW impact is described by the thermal conductivity equation with constant coefficients in the region of the heating source:

$$\frac{\partial T_e}{\partial t} - D_T \cos^2\theta \frac{\partial^2 T_e}{\partial z^2} + \delta\nu_e (T_e - T_0) = Q_T, \quad (3)$$

where $D_T = \frac{T_e}{m_e \nu_e} = \nu_e l_e^2$, $l_e = \frac{1}{\nu_e}\sqrt{\frac{T_e}{m_e}}$ is the mean free path of electrons; ν_e is the frequency of electron collisions; δ is the fraction of energy lost by an electron when it collides with a heavy particle (ion, neutral atom or molecule); Q (z, t) is the source characterizing the Joule heating of electrons by a high-frequency electric field (mainly plasma waves):

$$Q_T = \frac{2\sigma|\mathbf{E}|^2}{3N_0} \approx \frac{4W(z)}{3N_0}\frac{\nu_e}{8\pi}; \quad (4)$$

σ is the anti-Hermitian part of electron conductivity.

Turn now to the space-time structure of the sources $\Phi(z, t)$ and $Q_T(z, t)$. The domain of existence of plasma waves in Formulas (2) and (4) is characterized by the parameter Δz — the size of the heating source in height. According to theoretical models [Grach et al., 2016], plasma waves are concentrated in rather narrow regions of PW energy input to ionospheric plasma ($\Delta z\sim0.5$ km), i.e. near reflection $z=z_r$ and upper hybrid resonance $z=z_{uh}$ regions. The pondermotive parametric instability develops most rapidly (in a matter of milliseconds) near the reflection region, whereas near the UHR region the thermal parametric instability is excited more slowly,

and plasma waves develop for a few seconds (2–3 s) [Sergeev et al., 2016].

To simulate the development of perturbations of the electron density profile $\Delta N_e(z)$, we represent the spatial distribution of the sources $\Phi(z, t)$ and $Q_T(z, t)$ in the Gaussian form:

$$W(z) \propto e^{-\frac{(z-z_{uh})^2}{2\Delta z^2}} + \left(\frac{z_{uh}}{z_r}\right)^2 e^{-\frac{(z-z_r)^2}{2\Delta z^2}}, \quad (5)$$

with the same vertical size of the sources. The meaning of the multiplier $\left(\frac{z_{uh}}{z_r}\right)^2$ will be explained below. We suppose that plasma waves in the reflection region arise instantly, at zero second immediately after switching on a PW; whereas in the UHR region the plasma waves develop in ~2–3 s. Since the time of development of the thermal and pondermotive parametric instabilities is short compared to the time of temperature and electron density redistribution (see Equations (1), (3)), we assume that in the reflection region there is instantaneous excitation of plasma waves at t=0; and in the UHR region, with a delay Δt.

Let us assume $W(z)$ proportional to the pump wave intensity at the corresponding altitudes:

$$W(z) = \frac{\epsilon E_0^2(z)}{8\pi}, \quad (6)$$

where ϵ>>1 is the proportionality coefficient characterizing an increase in the real source associated with plasma waves, compared to the case when the source is only PW. Besides, the value of ϵ may differ for the sources associated with the pondermotive (at the point of reflection) and thermal parametric instabilities. Using both theoretical models and empirical data, Δz and ϵ can be estimated rather roughly; therefore, during the simulation the values of Δz and ϵ should vary in order to achieve acceptable agreement with empirical data.

Note that in experiments, where heating is carried out by an extraordinary wave, plasma waves are not excited. In this case, temperature should be calculated taking into account the distribution of the PW electric field over the entire region of the PW propagation. Here (for the case of heating by an ordinary wave), we limit ourselves to the finite size of the plasma wave generation region.

The PW electric field amplitude E_0 can be calculated by the formula [Gurevich, Schwarzburg, 1973]

$$E_0(z)[\text{В/м}] = 9.5\frac{\sqrt{P_0}\,[\text{Вт}]}{z[\text{м}]}, \quad (7)$$

where P_0 is the effective radiated power of the pump wave. Formula (5) has, therefore, a multiplier $\left(\frac{z_{uh}}{z_r}\right)^2$, associated with the spherical divergence of PW (the denominator z in Formula (7)).

The PW anomalous absorption in the UHR region, associated with the scattering of PW into plasma (UH) waves by small-scale irregularities elongated along the magnetic field, can lead, as already mentioned, to shielding of the reflection region and, accordingly, to suppression of the pondermotive parametric instability and a noticeable decrease in the depth of plasma expulsion at the reflection point. This situation took place in experiments both at the Sura facility [Shindin et al., 2012] and at the HAARP facility in the session at f_0=5500 MHz, conducted a few minutes later than that described in Section 1. This should lead to the $\epsilon(t)$ dependence when the upper hybrid turbulence develops. However, hereinafter for simplicity, in the simulation we ignore the anomalous attenuation effect and take ϵ to be identical for the reflection and UHR regions. Along with the plasma expulsion from the PW energy input regions there are competitive processes that, on the contrary, cause the electron density to increase in the PW energy input region. This is a disturbance of the ionization-recombination equilibrium owing to the dependence of the recombination coefficient on temperature [Gurevich, Schwarzburg, 1973; Benediktov et al., 1980; Boyko et al., 1985], as well as additional ionization of the ionospheric neutral component by electrons accelerated by plasma waves [Vaskov et al., 1981; Grach et al., 1998] up to the formation of reflecting layers [Bernhardt et al., 2016; Carlson, Jensen, 2014; Mishin et al., 2016; Pedersen et al., 2010; Pedersen et al., 2011; Sergeev et al., 2013]. Yet, these processes do not have such a pronounced spatial structure as the plasma expulsion in Figure 1. In the experiment [Shindin et al., 2021], an increase in the electron density due to the disturbance of the ionization-recombination equilibrium and, against its background, plasma expulsion were observed. At the same time, the formation of additional layers was not recorded because, first, the PW power was insufficient and, second, a vertical impact was made, while layers are effectively formed when the antenna pattern of the heating facility is directed to the magnetic zenith.

The existence of two plasma expulsion regions makes it possible to study the competition of two effects through simulation using Equations (1) and (3): plasma expulsion due to a gas- kinetic pressure increase by electron heating (the right-hand side of Equation (3) Q_T and the second term in the right-hand side of Equation (1)) and pondermotive plasma expulsion (the first term on the right-hand side of Equation (1)).

To figure out which of the mechanisms of formation of ionospheric plasma density regions prevails, we have carried out model calculations using Equations (1) and (3), taking the source for (2), (4), and (5). For the calculations, we took the following parameters: N_0=3.7·10^5 cm^{-3}, τ_N=30 s, T_0=2.07·10^{-13}erg (which corresponds to T_0=1500 K) — the initial electron temperature, ν_i=1 s^{-1}, P_0=175 MW, l_e=500 m, ν_e=300 s^{-1}, δ=10^{-4}.

To solve the ambipolar diffusion and thermal conductivity equations, we adopted the method of finite differences. The method involves changing the initial (continuous) problem of mathematical physics to its discrete analog (difference scheme). The domain of continuous change of arguments is replaced by a finite, or countable set of points, also known as nodes. The set of all nodes is called a net. Instead of functions of continu-

ous arguments, we analyze the so-called net functions defined on the net (in the net domain). The equations and conditions included in the description of the mathematical physics problem are replaced by their discrete analogs. The result is a net (difference) scheme. To tackle the elliptic problem by the method of finite differences, a net is constructed for the computational domain, then a difference scheme is selected and a difference equation is written for each node of the net (analog of the original equation but with the difference scheme), and thereafter boundary conditions are considered. A system of linear algebraic equations is taken whose solution yields approximate values in the nodes. Solving problems by the method of finite differences is an iterative process; at each iteration, we find a solution in a new time layer.

Note at the end of the section that the pondermotive expulsion and the Joule heating for a source located in the UHR region under stationary (prolonged) pumping have been analyzed in [Dimant, 1989]. The heating source $Q_T(z, t)$ was shown to be more significant for the formation of a lower-density region. This result has been confirmed by estimates made on the basis of the empirical data from [Grach et al., 1998].

3. NUMERICAL SIMULATION RESULTS

Figure 2–4 presents the results of simulation with (1), (3) for Δz=600 m and ϵ=6, at which the agreement between the calculated results and the experimental data seems to be the best. The half-width of the domain of existence of plasma waves Δz was chosen on the basis of existing theoretical concepts of plasma wave excitation in ionospheric experiments in the regions of reflection [Eliasson, 2013] and upper hybrid resonance [Grach et al., 1981; Grach et al., 2016] and was varied during the simulation within fairly narrow limits (~20–25 %); the value ϵ was selected for the best agreement between calculation results and empirical data (first of all, we are dealing with the maximum depths of electron density cavities $\Delta n_e/N_0$ at $z \sim z_r$ and $z \sim z_{uh}$).

Figure 2 illustrates the height distribution of electron temperature perturbations $\frac{\Delta T_e}{T_0} = \frac{T_e - T_0}{T_0}$ at 1, 3, 5, 15, 30, 40 s of heating. The position of the sources approximately corresponds to the heights of reflection and UHR in Figure 1. It is apparent that after the source is activated in the UHR region the electron temperature quickly equalizes in the interval between the reflection z_r and UHR z_{uh} heights, the regions of the PW energy input to ionospheric plasma. In this case, the second term on the right-hand side of Equation (1), responsible for the plasma expulsion caused by the gas-kinetic pressure increase due to electron heating (thermodiffusion source), weakly depends on z at $z_{uh} \lesssim z \lesssim z_r$.

Figure 3 for the same time points as in Figure 2 shows the relative electron density perturbation as a function of height $\frac{\Delta N_e}{N_0}(z,t) = \frac{N_e - N_0}{N_0}$, taking into account only the thermodiffusion source. It can be observed that due to

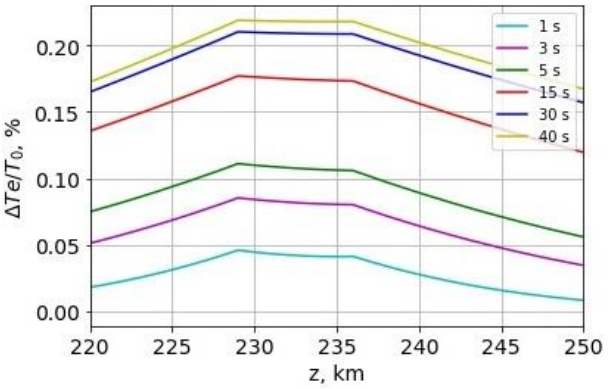

Figure 2. Relative increase in electron temperature as a function of height at various instants of time after switching on a PW.

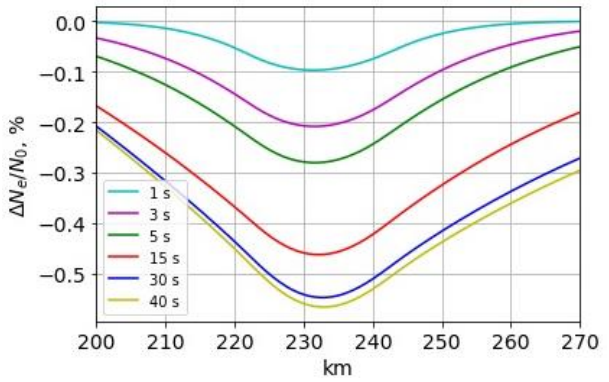

Figure 3. Relative variation in the electron density $\Delta N_e/N_0$ at plasma resonance heights of 230 km (UHR) and 237 km (reflection). Only the gas-kinetic pressure variation (i.e. the thermodiffusion source described by the second term in Equation (1)) is taken into account. Lines indicate the electron density dynamics at 1, 3, 5, 15, 30, and 40 s after switching on a PW

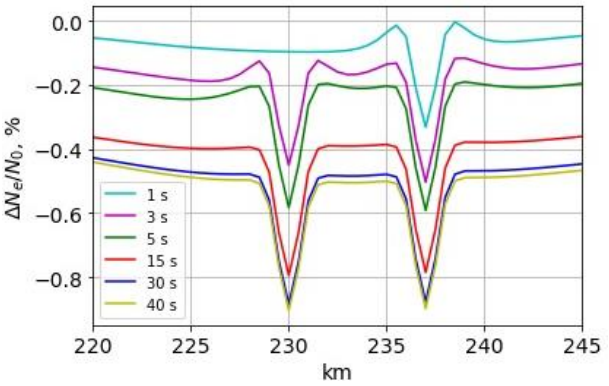

Figure 4. The same as in Figure 3 if both electron heating (the second term in Equation (1)) and pondermotive plasma expulsion (the first term in Equation (1)) are taken into account

the temperature equalization, thermal expulsion leads to the formation of a single electron density cavity at $z_{uh} \lesssim z \lesssim z_r$. There are no two spatially shifted regions at $z \sim z_r$ and in $z \sim z_{uh}$.

Figure 4 shows the dependence

$$\frac{\Delta N_e}{N_0}(z,t) = \frac{N_e - N_0}{N_0}$$

for the case of consideration of two sources — pondermotive and thermodiffusion — for the same plasma parameters as in Figures 2, 3. It can be seen that the behavior of $\Delta N_e/N_0$ in this Figure qualitatively corresponds to that observed in the experiment (see Figure 1) on modification of the electron density profile. First, a cavity develops near the reflection point, then, upon actuation of the thermal parametric instability, another cavity appears in the UHR region. These cavities are caused by the pondermotive plasma expulsion from the regions of PW energy contribution near z_r and z_{uh}. Later on, these two isolated cavities develop in parallel. Along with them, but more slowly, a more extended and shallow electron density cavity, associated with electron heating, develops.

Thus, we may conclude that when lower-density regions are formed in the plasma resonance region, regardless of two or one, both effects (the gas-kinetic (thermodiffusion) plasma expulsion due to electron heating and the pondermotive plasma expulsion) should play the role. Specifically, the pondermotive plasma expulsion is responsible for the local location of the lower-density regions observed in the experiments near the heights of plasma resonances. The total depth of the cavities is determined by the additive effect of thermal and pondermotive expulsions. Note that this conclusion does not depend on the specific values of Δz and ϵ, used for the simulation and typical for experimental conditions.

4. DISCUSSION

The purpose of this work was to determine the mechanism of formation of the modified electron density profile, observed in the experiment at the HAARP facility, in the ionosphere under the action of a powerful HF radio wave [Shindin et al., 2021]. The model for the vertical distribution of the energy density of plasma waves excited by the impact differs in a number of parameters from the distribution that actually exists in the experiment. First, we take almost identical distribution of $W(z)$ at $z\sim z_r$ and $z\sim z_{uh}$. In fact, the widths of the Δz regions occupied by plasma waves, the form of the dependence $W(z)$, the intensity of plasma waves in each specific pumping session are unknown. Theoretical calculations [Eliasson, 2013; Grach et al., 2016] do not give a full answer to this question either. In most experiments, especially when the frequency of a powerful wave did not approach the multiple gyroresonance frequencies, there was a decrease or complete disappearance of plasma expulsion from the $z\sim z_r$ region, associated with the consuming PW energy (shielding of the reflection region) at altitudes $z\sim z_{uh}$ due to the anomalous absorption. Such an effect occurs in experiments at SURA and HAARP facilities; in the latter case the PW frequency was f_0=5500 kHz [Shindin et al., 2012; Sergeev et al., 2016]. The two isolated expulsion regions were most clearly pronounced at $4 f_{H_e} > f_0 \geq 5540$ kHz.

The development of the cavities after switching on a PW is described in more detail in [Shindin et al., 2021]. Interpreting the occurrence of two isolated cavities in the PW frequency range $f_0 \lesssim 4 f_{He}$ is beyond the scope of this work and requires more advanced and detailed models of the development of artificial ionospheric turbulence.

Nevertheless, from the simulation of the electron density profile formation during the PW energy input to ionospheric plasma in the $z\sim z_r$ and $z\sim z_{uh}$ regions using Equations (1) and (3), we have found that there is a qualitative agreement between the simulation results and the experimental data when taking into account both thermal and pondermotive plasma expulsion from PW energy input regions: first, local cavities of electron density appear near the regions of the PW energy input to plasma at $z\sim z_r$ and $z\sim z_{uh}$ due to the pondermotive plasma expulsion; then a more extended electron density cavity associated with electron heating develops. We may, therefore, consider it established that the decisive role in the presence of two lower electron density regions is played by the pondermotive plasma expulsion from the plasma resonance regions. The total decrease in plasma density in plasma resonance regions is determined by the additive effect of thermal and pondermotive expulsion.

The work was financially supported by RSF Grants No. 20-12-000197 (development of the theoretical model, analysis of the results) and No. 21-72-10131 (numerical solution of Equations (1), (3)).

REFERENCES

Benediktov E.A., Getmantsev G.G., Zyuzin V.A., Ignatiev Yu.A. Heating of the E-region of the ionosphere by powerful short-wave radio emission. *Geomagnetism and Aeronomy*. 1980, vol. 20, iss. 5, pp. 955–956, (In Russian).

Berezin I.V., Belyansky V.B., Budko N.I., Vaskov V.V., Dimant Y.S., Zyuzin V.A., et al. Diagnostics of the process of excitation of plasma oscillations by the field of a powerful radio wave, *Geomagnetism and Aeronomy*. 1991, vol. 31, iss. 5, pp. 874–880. (In Russian).

Bernhardt P.A., Siefring C.L., Briczinski S.J., McCarrick M., Michell R.G. Large ionospheric disturbances produced by the HAARP HF facility. *Radio Sci*. 2016, vol. 51, iss. 7, pp. 1081–1093. DOI: 10.1002/ 2015RS005883.

Boyko G.N., Vaskov V.V., Golyan S.F., Gurevich A.V., Dimant Ya.S., Zyuzin V.A., et al. Study of defocusing of radio waves under the influence of high-power radio emission. *Izv. Vuz. Radiophysics.* 1985, vol. 28, iss. 8, pp. 960–970. (In Russian).

Carlson H.C., Jensen J.B. HF accelerated electron fluxes, spectra, and ionization. *Earth, Moon, and Planets*. 2014. vol. 116, pp. 1–18. DOI: 10.1007/ s11038-014-9454-6.

Dimant Ya.S. Thermal and striction perturbation of the ionospheric plasma density in the resonance region of a powerful radio wave. *Vzaimodeistvie vysokochastotnykh voln s ionosferoi* [Interaction of HF Waves with the Ionosphere]. Moscow, IZMIRAN Publ., 1989, pp. 19–39. (In Russian).

Eliasson B. Full-scale simulations of ionospheric Langmuir turbulence. *Modern Physics Letters B.* 2013, vol. 27, no. 08, pp. 1330005–1330005-27. DOI: 10.1142/S0217984913300056.

Gaponov A.V., Miller M.A. On potential wells for charged particles in high-frequency fields. *JETP Letters*. 1958, vol. 34, no. 2, pp. 242–243. (In Russian).

Grach S.M., Trakhtengerts V.Yu. On the parametric excitation of ionospheric inhomogeneities elongated along the magnetic field. *Izvestiya vuzov. Radiophysics*. 1975, vol. 18, pp. 1288–1296. (In Russian).

Grach S.M., Mityakov N.A., Rapoport V.O., Trakhtengertz V.Yu. Thermal parametric turbulence in a plasma. *Physica D: Nonlinear Phenomena*. 1981, vol. 2, pp. 102–106. DOI: 10.1016/0167-2789(81)90063-4.

Grach S.M., Mityakov N.A., Schwartz M.M. Plasma density jump at the advanced stage of thermal parametric instability. *Geomagnetism and Aeronomy*. 1989, vol. 29, iss. 4, pp. 590–596. (In Russian).

Grach S.M., Komrakov G.P., Yurishchev M.A., Thide B., Leyser T.B., Carozzi T. Multifrequency Doppler radar observation of electron gyroharmonic effects during electromagnetic pumping of the ionosphere. *Phys. Rev. Lett.* 1997, vol. 78, pp. 883–886. DOI: 10.1103/PhysRevLett.78.883.

Grach S.M., Komrakov G.P., Schwartz M.M., Yurishchev M.A. On the dependence of the anomalous attenuation of probe waves on frequency under the influence of powerful radio emission on the ionosphere. *Izvestiya vuzov. Radiophysics*. 1998, vol. 41, pp. 678–966. (In Russian).

Grach S.M., Sergeev E.N., Mishin E.V., Shindin A.V. Dynamic properties of ionospheric plasma turbulence driven by high-power high-frequency radiowaves. *Physics-Uspekhi*. 2016, vol. 59, no. 11, pp. 1091–1128. DOI: 10.3367/UFNe.2016. 07.037868.

Gurevich A.V., Schwarzburg A.B. *Nelineinaya teoriya rasprostraneniya radiovoln v ionosfere* [Nonlinear Theory of Radio Wave Propagation in the Ionosphere]. Moscow, Nauka Publ., 1973, 272 p. (In Russian).

Lobachevsky L.A., Gruzdev Yu.V., Kim V.Yu., Mikhaylova G.A, Panchenko V.A., Polimatidi V.P., et al. Observations of ionospheric modification by the Tromsø heating facility with the mobile diagnostic equipment of IZMIRAN. *J. Atmos. Terr. Phys*. 1992, vol. 54, iss. 1. pp. 75–85. DOI: 10.1016/0021-9169(92)90086-Z.

Mishin E., Watkins B., Lehtinen N., Eliasson B., Pedersen T., Grach S.M. Artificial ionospheric layers driven by high-frequency radiowaves: An assessment. *J. Geophys. Res. Space Phys.* 2016, vol. 121, pp. 3497–3524. DOI: 10.1002/2015JA021823.

Pedersen T., Gustavsson B., Mishin E., Kendall E., Mills T., Carlson H.C., Snyder A.L. Creation of artificial ionospheric layers using high-power HF waves. *Geophys. Res. Lett.* 2010, vol. 37, L02106. DOI: 10.1029/2009GL041895.

Pedersen T., McCarrick M., Reinisch B., Watkins B., Hamel R., Paznukhov V., Production of artificial ionospheric layers by frequency sweeping near the 2nd gyroharmonic. *Ann. Geophys.* 2011, vol. 29, pp. 47–51.

Pitaevskii L.P. Electric forces in a transparent medium with dispersion. *JETP Letters*. 1960, vol. 39, pp. 1450–1458. (In Russian).

Sergeev E.N., Grach S.M., Kotov P.V., Komrakov G.P., Boyko G.N., Tokarev Yu.V. Diagnostics of the disturbed ionospheric region using broadband radio emission. *Radiophysics*. 2007, vol. 50, pp. 649–668. (In Russian).

Sergeev E.N., Grach S.M., Shindin A.V., Mishin E., Bernhardt P.A., Briczinski S., et al. Artificial ionospheric layers during pump frequency stepping near the 4th gyroharmonic at HAARP. *Phys. Rev. Lett.* 2013, vol. 110, 065002. DOI: 10.1103/PhysRevLett.110.065002.

Sergeev E.N., Shindin A.V., Grach S.M., Milikh G.M., Mishin E.V., Bernhardt P.A., et al. Exploring HF-induced ionospheric turbulence by Doppler sounding and stimulated electromagnetic emissions at the High Frequency Active Auroral Research Program heating facility. *Radio Sci.* 2016, vol. 51, pp. 1118–1130. DOI: 10.1002/2015RS005936.

Shindin A., Sergeev E., Grach S. Applications of broadband radio signals for diagnostics of electron density profile dynamics and plasma motion in the HF-pumped ionosphere. *Radio Sci.* 2012, vol. 47, RS0N04. DOI: 10.1029/2011RS004895.

Shindin A.V., Sergeev E.N., Grach S.M., Milikh G.M., Bernhardt P.A., Siefring C., McCarrick M.J. HF Induced modifications of the electron density profile in the Earth's ionosphere using the pump frequencies near the fourth electron gyroharmonic. *Remote Sensing*. 2021, vol. 13, 4895. DOI: 10.3390/rs13234895.

Vaskov V.V., Dimant Ya.S. Influence of deformation of the normal profile of the ionospheric plasma on the anomalous absorption of a powerful radio wave in the resonant region, *Geomagnetism and Aeronomy*. 1989, vol. 29, pp. 373–377. (In Russian).

Vas'kov V.V., Gurevich A.V. Nonlinear resonant instability of a plasma in the field of an ordinary electromagnetic wave. *Sov. Phys. —·JETP.* 1976, vol. 42, iss. 1, pp. 91–97.

Vaskov V.V., Golyan S.F., Gruzdev Yu.V., Gurevich A.V., Dimant Y.S., Kim V.Yu., et al. Stimulated ionization of the upper ionosphere during the interaction of a powerful radio wave. *JETP Lett.* 1981, vol. 34, no. 11, pp. 582–585. (In Russian).

Vaskov V.V., Golyan S.F., Gurevich A.V., Dimant Ya.S., Zyuzin V.A., Kim V.Yu., et al. Excitation of an upper hybrid resonance in an ionospheric plasma by a powerful radio wave fiel. *JETP Lett*. 1986, vol. 43, no. 11, pp. 512–515. (In Russian).

This paper is based on material presented at the 17th Annual Conference on Plasma Physics in the Solar System, February 7–11, 2022, IKI RAS, Moscow.

Original Russian version: Legostaeva Yu.K., Shindin A.V., Grach S.M., published in Solnechno-zemnaya fizika. 2022. Vol. 8. Iss. 3. P. 74–81. DOI: 10.12737/szf-83202211.

How to cite this article

Legostaeva Yu.K., Shindin A.V., Grach S.M. Response of ionospheric electron density profile to the action of powerful HF radiowave radiation. *Solar-Terrestrial Physics*. 2022. Vol. 8. Iss. 3. P. 69–75. DOI: 10.12737/stp-83202211.